96-49

Verrelst H., Van Acker K., Suykens J.A.K., Motmans B., De Moor B., Vandewalle J., "NL_q neural control theory: case study for a ball and beam system", in *Proc. of the European Control Conference (ECC'97)*, Brussels, Belgium, Jul. 1997., Lirias number: 179603.

NL_q neural control theory: case study for a ball and beam system*

H. Verrelst, K. Van Acker, J. Suykens, B. Motmans, B. De Moor, J. Vandewalle

Katholieke Universiteit Leuven, Dept. of Electr. Eng., ESAT-SISTA
Kardinaal Mercierlaan 94, B-3001 Leuven (Heverlee), Belgium
Tel: 32/16/32 11 11 Fax: 32/16/32 19 86
E-mail: herman.verrelst,johan.suykens,bart.demoor,joos.vandewalle@esat.kuleuven.ac.be

Keywords: Neural nets

Abstract

In this paper we design a linear dynamic output feedback controller for a ball and beam system based on an identified neural state space model. This is done by applying dynamic backpropagation, constrained by NL_q internal or I/O stability conditions. The performance of the controller has been tested on a real ball and beam set-up.

1 Introduction

A widely used algorithm in neural model based controller design is Narendra's dynamic backpropagation procedure [6]. Training is done then by means of optimising a cost function which is based on the controller's tracking performance, defined on a set of specific reference inputs. This method however doesn't assure proper generalisation to reference inputs outside the training set, nor can it guarantee closed-loop internal or I/O stability stability. Recent work of Suykens *et al.* [7][9] has introduced criteria for internal and I/O stability based on the so-called NL_q representation of the closed-loop system. The NL_q theory enables a top-down linear or neural controller design for general non-linear systems, based on identified neural state space models. In this paper we present a case study for a ball and beam system. Controllers are designed by means of Narendra's dynamic backpropagation procedure, modified with NL_q stability criteria. It will be shown that weaknesses of classical dynamic backpropagation can be overcome to produce controllers of a quality comparable to for example LQG controllers for this system.

This paper is organised as follows. In Section 2 we present the ball and beam system and its identification using a neural state space model. In Section 3 the controller and reference model are shown and the closed-loop equations are rewritten in an NL_q representation. The NL_q criteria for closed-loop internal and I/O stability are described in Section 4. Section 5 discusses the controller design using classical dynamic backpropagation. Section 6 demonstrates how the NL_q criteria can be used in the controller design and shows the validation of the controllers during tests on the real ball and beam system.

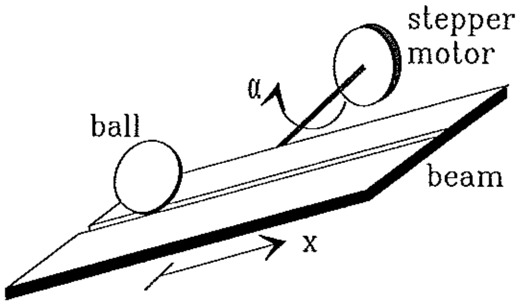

Figure 1: Ball and beam set-up.

2 Identification of the ball/beam using neural state space models

The system to be controlled (Fig. 1) consists of a beam on which a rolling ball has to be stabilised and positioned [4]. The control action is performed by a stepper motor that sets the angular position of the beam. The position

*This research work was carried out at the ESAT laboratory and the Interdisciplinary Center of Neural Networks ICNN of the Katholieke Universiteit Leuven, in the framework of the Belgian Programme on Interuniversity Poles of Attraction, initiated by the Belgian State, Prime Minister's Office for Science, Technology and Culture (IUAP-17, IUAP-50) and in the framework of a Concerted Action Project MIPS (Modelbased Information Processing Systems) of the Flemish Community, ICCoS (Identification and Control of Complex Systems), Human Capital and Mobility Network (SIMONET) and SCIENCE-ERNSI (SC1-CT92-0779).

of the ball relative to the middle of the beam is taken as the output (in meters) and is measured by means of a potentiometer system attached to the beam.

First the dynamic relation between the angle of the beam and the velocity of the ball was described in a deterministic neural state space model [8]. An integrator is added to obtain a complete angle-to-position model of the form

$$\left\{ \begin{array}{rcl} \hat{x}_{k+1} & = & W_{AB} \tanh(V_A \hat{x}_k + V_B u_k) \\ \hat{v}_k & = & W_{CD} \tanh(V_C \hat{x}_k + V_D u_k) \\ \hat{s}_{k+1} & = & \hat{s}_k + \frac{1}{f_s} \hat{v}_k \\ \hat{y}_k & = & \hat{s}_k, \end{array} \right. \quad (1)$$

where f_s is the sampling frequency (10 Hz), the state is $\hat{x}_k \in \mathbb{R}^{n_x}$, the velocity $\hat{v}_k \in \mathbb{R}^l$, the integrator state $\hat{s}_k \in \mathbb{R}^l$, the position $\hat{y}_k \in \mathbb{R}^l$ and the input signal $u_k \in \mathbb{R}^m$, with $m = l = 1$ and $n_x = 2$. The interconnection matrices in the neural state space model are $W_{AB} \in \mathbb{R}^{n_x \times n_{h_x}}$ $V_A \in \mathbb{R}^{n_{h_x} \times n_x}$, $V_B \in \mathbb{R}^{n_{h_x} \times m}$, $W_{CD} \in \mathbb{R}^{l \times n_{h_v}}$, $V_C \in \mathbb{R}^{n_{h_v} \times n_x}$, $V_D \in \mathbb{R}^{n_{h_v} \times m}$, with n_{h_x} and n_{h_v} the number of hidden neurons in the velocity model.

Using a priori knowledge by imposing the integrator in the model is done because the intrinsic instability of the system makes I/O-measurements difficult and obtained data doesn't contain enough information to model the underlying behaviour.

Learning of the neural state space model was based on numerically differentiated output data and was done using a prediction error algorithm. Dynamic backpropagation was used with a Narendra sensitivity model [6] for calculation of the gradient of the cost function. A quasi-Newton method has been used for local optimisation [5]. Starting values for the model parameters were derived from linear ARX models [7] and the numbers of hidden neurons were chosen as $n_{h_x} = 2$ and $n_{h_v} = 1$. The neural velocity model has been successfully validated by means of higher order correlation tests [1][8].

3 Control scheme and its NL_q representation

In order to design a controller based on the identified model (1), a linear dynamic output feedback controller is taken of the form

$$\left\{ \begin{array}{rcl} z_{k+1} & = & E z_k + F \hat{y}_k + F_2 r_k \\ u_k & = & G z_k + H \hat{y}_k + H_2 r_k, \end{array} \right. \quad (2)$$

where $z_k \in \mathbb{R}^{n_z}$ is the controller state, $u_k \in \mathbb{R}^m$ the model input, $\hat{y}_k \in \mathbb{R}^l$ the output and $r_k \in \mathbb{R}^l$ the reference signal. The following specific structure is taken for this controller:

$$\begin{array}{rcl} E & = & \begin{bmatrix} Q_1 & Q_2 \\ 0 & 1 \end{bmatrix}, \\ F & = & \begin{bmatrix} Q_3 \\ -1 \end{bmatrix}, \quad F_2 = \begin{bmatrix} Q_4 \\ 1 \end{bmatrix}, \\ G & = & \begin{bmatrix} Q_5 & Q_6 \end{bmatrix}, \\ H & = & \begin{bmatrix} 0 \end{bmatrix}, \quad H_2 = \begin{bmatrix} Q_7 \end{bmatrix}, \end{array} \quad (3)$$

In this way integral control is obtained and steady state errors are avoided.

A reference model with a low pass filter characteristic is introduced, with state space representation

$$\left\{ \begin{array}{rcl} \mu_{k+1} & = & A_r \mu_k + B_r d_k \\ r_k & = & C_r \mu_k, \end{array} \right. \quad (4)$$

where $A_r \in \mathbb{R}^{n_f \times n_f}$, $B_r \in \mathbb{R}^{n_f \times l}$, $C_r \in \mathbb{R}^{l \times n_f}$, n_f is the order of the reference model, μ_k is the state, d_k the input of the reference model. A cut-off frequency of 5 Hz was chosen.

The closed-loop system is shown in Fig. 2. For the regulated output both the relatively weighted control signal ρu_k and the tracking error $r_k - \hat{y}_k$ are considered.

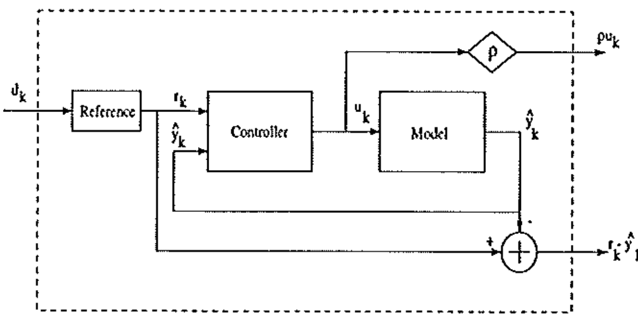

Figure 2: Closed-loop system

The equations for the closed-loop system are

$$\left\{ \begin{array}{rcl} \hat{x}_{k+1} & = & W_{AB} \sigma(V_A \hat{x}_k + V_B(G z_k + H_2 \mu_k)) \\ \hat{s}_{k+1} & = & \hat{s}_k + \frac{1}{f_s} W_{CD} \sigma(V_C \hat{x}_k + V_D(G z_k + H_2 \mu_k)) \\ z_{k+1} & = & E z_k + F \hat{s}_k + F_2 C_r \mu_k \\ \mu_{k+1} & = & A_r \mu_k + B_r d_k \\ r_k - \hat{y}_k & = & C_r \mu_k - \hat{s}_k \\ \rho u_k & = & \rho G z_k + \rho H_2 C_r \mu_k. \end{array} \right. \quad (5)$$

After introduction of the following new state variables

$$\begin{array}{rcl} \xi_k & = & \sigma(V_A \hat{x}_k + V_B G z_k + V_B H_2 C_r \mu_k) \\ \eta_k & = & \sigma(V_C \hat{x}_k + V_D G z_k + V_D H_2 C_r \mu_k), \end{array} \quad (6)$$

these equations can be rewritten in the standard plant NL_1 representation [2][7][9]

$$\left\{ \begin{array}{rcl} p_{k+1} & = & \Gamma_1(V_1 p_k + B_1 w_k) \\ e_k & = & \Lambda_1(W_1 p_k + D_1 w_k) \end{array} \right. \quad (7)$$

with state vector $p_k = [\hat{x}_k; \hat{s}_k; z_k; \mu_k; \xi_k; \eta_k]$, regulated output $e_k = [r_k - \hat{y}_k; \lambda u_k]$, exogenous input $w_k = d_k$ and

$$V_1 = \begin{bmatrix} 0 & 0 & 0 & 0 & W_{AB} & 0 \\ 0 & I & 0 & 0 & 0 & \frac{1}{f_s}W_{CD} \\ 0 & F & E & F_2C_r & 0 & 0 \\ 0 & 0 & 0 & A_r & 0 & 0 \\ 0 & V_BGF & V_BGE & V_BGF_2C_r + F_2C_rA_r & V_AW_{AB} & 0 \\ 0 & V_DGF & V_DGE & V_DGF_2C_r + F_2C_rA_r & V_CW_{AB} & 0 \end{bmatrix},$$

$$B_1 = \begin{bmatrix} 0 \\ 0 \\ 0 \\ B_r \\ 0 \\ 0 \end{bmatrix}, \quad W_1 = \begin{bmatrix} 0 & -I & 0 & C_r & 0 & 0 \\ 0 & 0 & \rho G & \rho H_2 C_r & 0 & 0 \end{bmatrix}, \quad D_1 = \begin{bmatrix} 0 & 0 \\ 0 & 0 \end{bmatrix}.$$

This is a special case ($q = 1$) of the general NL_q representation [7][9]

$$\begin{cases} p_{k+1} = \Gamma_1(V_1\Gamma_2(V_2 \ldots \Gamma_q(V_q p_k + B_q w_k) \ldots + B_2 w_k) + B_1 w_k) \\ e_k = \Lambda_1(W_1\Lambda_2(W_2 \ldots \Lambda_q(W_q p_k + D_q w_k) \ldots + D_2 w_k) + D_1 w_k). \end{cases} \quad (8)$$

4 NL_q stability criteria

For the case of internal stability of the closed-loop system, the NL_q representation (8) becomes

$$p_{k+1} = (\prod_{i=1}^{q} \Gamma_i(p_k)V_i)p_k. \quad (9)$$

In this case the state vector can be simplified to $p_k = [\hat{x}_k; \hat{s}_k; z_k; \xi_k; \eta_k]$, without the state μ_k of the reference model. The NL_q (9) becomes

$$p_{k+1} = \Gamma_1(p_k)V_1^{(a)}p_k \quad (10)$$

with

$$V_1^{(a)} = \begin{bmatrix} 0 & 0 & 0 & W_{AB} & 0 \\ 0 & I & 0 & 0 & \frac{1}{f_s}W_{CD} \\ 0 & F & E & 0 & 0 \\ 0 & V_BGF & V_BGE & V_AW_{AB} & 0 \\ 0 & V_DGF & V_DGE & V_CW_{AB} & 0 \end{bmatrix},$$

where $V_1^{(a)} \in \mathbb{R}^{n_v \times n_v}$, with $n_v = n_x + l + n_z + n_{h_z} + n_{h_y}$. According to [7] a sufficient condition for global asymptotic stability of the autonomous NL_1 system (10) is to find a matrix $P_1 \in \mathbb{R}^{n_v \times n_v}$ such that

$$\kappa(P_1)\ \|P_1 V_1^{(a)} P_1^{-1}\|_2 < 1 \quad (11)$$

where $\kappa(P_1) = \|P_1\|_2 \|P_1^{-1}\|_2$. This criterion for global asymptotic stability can be restated as a condition for local stability at the origin

$$\min \kappa(P_1) \quad s.t. \quad \|P_1 V_1^{(a)} P_1^{-1}\|_2 < 1, \quad (12)$$

whereby minimising $\kappa(P_1)$ enlarges the region of attraction at the origin. For the more general formulation in the case $q > 1$, we refer to [7][9].

I/O stability criteria for NL_qs [7] make use of the following equivalent closed-loop system representations for (8):

$$\begin{cases} p_{k+1} = (\prod_{i=1}^{q} \Gamma_{i,e}(p_k, w_k)M_i) \begin{bmatrix} p_k \\ w_k \end{bmatrix} \\ e_k = (\prod_{i=1}^{q} \Lambda_{i,e}(p_k, w_k)N_i) \begin{bmatrix} p_k \\ w_k \end{bmatrix} \end{cases} \quad (13)$$

with

$$\Gamma_{1,e} = \Gamma_1 \qquad \Gamma_{i,e} = \begin{bmatrix} \Gamma_i & 0 \\ 0 & I \end{bmatrix}$$

$$M_1 = \begin{bmatrix} V_1 & B_1 \end{bmatrix} \qquad M_i = \begin{bmatrix} V_i & B_i \\ 0 & I \end{bmatrix}$$

$$\Lambda_{1,e} = \Lambda_1 \qquad \Lambda_{i,e} = \begin{bmatrix} \Lambda_i & 0 \\ 0 & I \end{bmatrix}$$

$$N_1 = \begin{bmatrix} W_1 & D_1 \end{bmatrix} \qquad N_i = \begin{bmatrix} W_i & D_i \\ 0 & I \end{bmatrix}$$

$$(i = 2, \ldots, q)$$

and

$$\begin{bmatrix} p_{k+1} \\ e_k \end{bmatrix} = (\prod_{i=1}^{q} \Omega_i(p_k, w_k^{ext})R_i) \begin{bmatrix} p_k \\ w_k^{ext} \end{bmatrix} \quad (14)$$

with

$$\Omega_i = \begin{bmatrix} \Gamma_{i,e} & 0 & 0 \\ 0 & \Lambda_{i,e} & 0 \end{bmatrix}, \quad R_i = \begin{bmatrix} M_i & 0 & 0 \\ 0 & N_i & 0 \end{bmatrix},$$

$$R_q = \begin{bmatrix} M_q & 0 \\ N_q & 0 \end{bmatrix}, \qquad (i = 1, \ldots, q-1)$$

where w_k^{ext} consists of the input u_k extended with a fictitious input signal in order to make $\prod_{i=1}^{q} R_i$ square. This additional input may be interpreted here as a noise input, which is considered to be zero because of the purely deterministic model.

For the NL_1 (7) the representation (14) reduces to

$$\begin{bmatrix} p_{k+1} \\ r_k - \hat{y}_k \\ \lambda u_k \end{bmatrix} = \Omega_1(p_k, d_k)R_1 \begin{bmatrix} p_k \\ d_k \\ 0 \end{bmatrix}, \quad (15)$$

with

$$R_1 = \begin{bmatrix} V_1 & B_1 & 0 \\ W_1 & D_1 & 0 \end{bmatrix},$$

where $R_1 \in \mathbb{R}^{n_r \times n_r}$, with $n_r = n_x + l + n_z + n_f + n_{h_z} + n_{h_y} + l + l$.

The following condition [7] guarantees I/O stability with finite L_2-gain for the NL_1 system (15). If there exists a matrix P_{S_1} =blockdiag$\{P_1, \delta I_{2l}\}$ with $P_1 \in \mathbb{R}^{n_v \times n_v}$ and δ a real scalar, such that

$$c_P \beta_P < 1 \qquad (16)$$

with $c_P = \kappa(P_{S_1})$ en $\beta_P = \|P_{S_1} R_1 P_{S_1}^{-1}\|_2$, then there exists a positive constant c_1 such that

$$\|e\|_2^2 \leq c_P^2 \beta_P^2 \|w\|_2^2 + c_1 \|p_0\|_2^2. \qquad (17)$$

when $\{w_k\}_{k=0}^{\infty} \in l_2$. In analogy with the internal stability case (12), one considers

$$\min c_P = \kappa(P_{S_1}) \quad s.t. \quad \|P_{S_1} R_1 P_{S_1}^{-1}\|_2 < 1. \qquad (18)$$

The conditions (12) and (18) can also be expressed as LMIs (Linear Matrix Inequalities) [3][7].

5 Classical dynamic backpropagation

In classical neural control using Narendra's dynamic backpropagation [6], one trains a controller by optimizing on a set of specific reference inputs by solving the parametric optimisation problem

$$\min_{\theta_c} J(\theta_c) = \frac{1}{2N} \sum_{k=1}^{N} \{[r_k - \hat{y}_k(\theta_c)]^T [r_k - \hat{y}_k(\theta_c)] + \lambda u_k(\theta_c)^T u_k(\theta_c)\} \qquad (19)$$

where θ_c is the controller parameter vector, N is the time horizon and λ a positive constant.

For the ball and beam we trained the controller on a step reference input. For the optimisation algorithm we applied a quasi-Newton method, with BFGS update of the Hessian [5]. The gradient of the cost function was calculated numerically.

The instability of the ball and beam system limits the length of time horizons in the cost function (19). Therefore we have taken $N = 50$ (5*sec.*) as shown on Fig. 3. Starting from random initial controller parameter vectors, the optimisation leads to bad results in the sense that a closed-loop system is obtained in which the origin is unstable and multiple equilibrium points appear. Also poor generalisation outside the training set is observed. Typical simulation results are shown on Fig. 3 and Fig. 4.

In general one can say that a controller design solely based on optimisation of the cost function (19) cannot guarantee closed-loop stability nor proper generalisation to reference inputs outside the training set. In the next Section we show how this problem can be avoided by applying NL_q stability constraints.

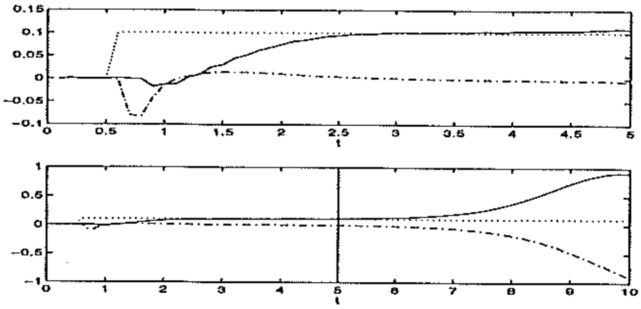

Figure 3: Simulation of the closed-loop behaviour shows that, when using classical dynamic backpropagation, the tracking error is small on the training interval (5*sec.*, before the vertical line on bottom figure), but that the generalisation outside the interval is bad (r_k: $\cdots$; u_k: -.-; $\hat{y}_k$: –).

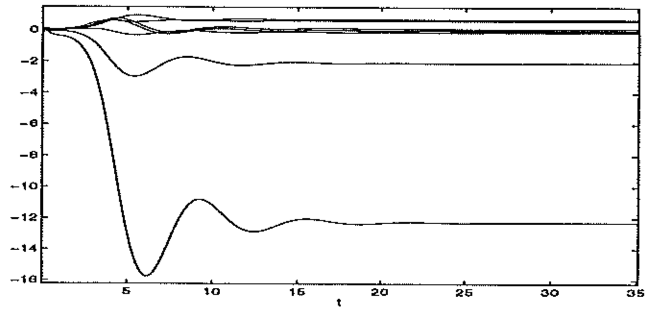

Figure 4: The simulated behaviour of the autonomous closed-loop system for a randomly chosen initial state vector. The closed-loop system has unwanted multiple equilibria in case one applies classical dynamic backpropagation.

6 Dynamic backpropagation with NL_q stability constraints

In order to guarantee closed-loop and I/O stability, we modify Narendra's dynamic backpropagation with NL_q stability constraints [7].

6.1 Internal stability constraint

The optimisation problem (19) is modified using criterion (12) in order to impose internal closed-loop stability. This results into

$$\min_{\theta_c, P_1} J(\theta_c) \quad s.t. \quad \begin{cases} \|P_1 V_1^{(a)}(\theta_c) P_1^{-1}\|_2 < 1 \\ \kappa(P_1) < \alpha, \end{cases} \qquad (20)$$

where $J(\theta_c)$ is defined in (19) and α is a user-defined upper-bound on the condition number $\kappa(P_1)$.

Using SQP (Sequential Quadratic Programming) [5] in order to solve (20), a better formulation of the problem turned out to be

$$\min_{\theta_c, P_1} \|P_1 V_1^{(a)}(\theta_c) P_1^{-1}\|_2 \quad s.t. \quad \begin{cases} J(\theta_c) < \beta \\ \kappa(P_1) < \alpha, \end{cases} \qquad (21)$$

where β is a user-defined upper-bound on the tracking error.

Starting from random initial parameter vectors, the problem was solved for $\alpha = 200$ and $\beta = 0.13$ and with the same specifications on the cost function (19) as in Section 5: step reference input, $N = 50$ (5*sec.*). The identity matrix was taken as the starting point for P_1. The obtained controllers were found to be locally stable and by lowering the upper bound on $\kappa(P_1)$ to $\alpha = 80$ the region of attraction could be extended over the entire working range of the ball and beam system. Fig. 5 shows the simulation of the autonomous closed-loop with a controller for which $\|P_1 V_1^{(a)}(\theta_c) P_1^{-1}\|_2 = 0.97$ and $\kappa(P_1) = 75$.

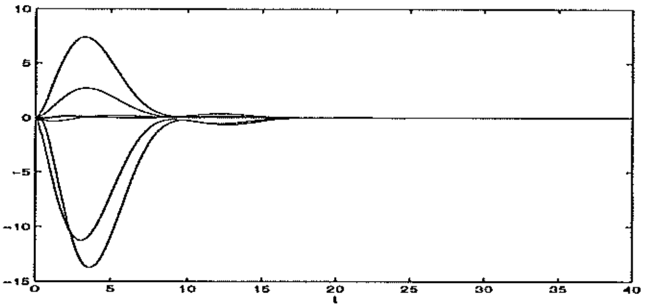

Figure 5: Using the NL_q constraint, internal stability is successfully imposed on the closed-loop system. When initialised with values randomly spread over the entire working range of the ball and beam system, all trajectories converge to the origin.

Also the controller's tracking performance and generalisation to other signals has improved as shown in Fig. 6.

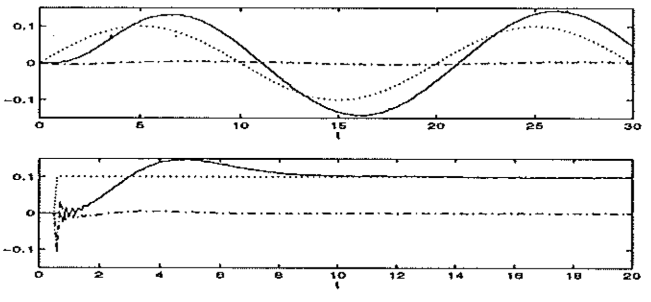

Figure 6: Using the NL_q internal stability constraint, the controller's generalisation outside the training interval of Fig. 3 and to other reference inputs (top: sine input) is better when compared to classical dynamic backpropagation (r_k:$\cdots$; u_k:-.-; $\hat{y}_k$: –).

6.2 I/O stability constraint

Modification of the optimisation problem (19) by means of the NL_q I/O stability constraint (18), gives

$$\min_{\theta_c, P_{S_1}} J(\theta_c) \quad s.t. \quad \begin{cases} \|P_{S_1} R_1(\theta_c) P_{S_1}^{-1}\|_2 < 1 \\ \kappa(P_{S_1}) < \alpha. \end{cases} \tag{22}$$

Here the cost function has been redefined as

$$J(\theta_c) = \max_{T_r < k < N} r_k - \hat{y}_k, \tag{23}$$

where r_k is step reference signal and T_r is a user-defined upper-bound on the rise time. Using this cost function a better closed-loop system performance has been obtained.

Like for the internal stability case (20), this optimisation problem was solved by means of SQP as

$$\min_{\theta_c, P_{S_1}} \|P_{S_1} R_1(\theta_c) P_{S_1}^{-1}\|_2 \quad s.t. \quad \begin{cases} J(\theta_c) < \beta \\ \kappa(P_{S_1}) < \alpha. \end{cases} \tag{24}$$

With the specifications $T_r = 2sec.$, $\beta = 1cm$ and $\alpha = 100$ and again starting from random parameter vectors and taking the identity matrix for the starting point of P_1, we obtained controllers that show improved generalisation to other reference signals and are comparable in performance with LQG controllers [3] for the ball and beam system. This is illustrated in Fig. 7, 8 and 9, where we show output and control signal as measured on the real ball and beam system, when testing a controller for which $\|P_{S_1} R_1(\theta_c) P_{S_1}^{-1}\|_2 = 0.98$ and $\kappa(P_{S_1}) = 86$.

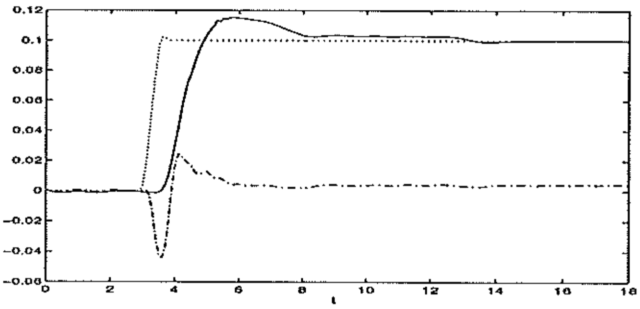

Figure 7: Step response as measured on the real ball and beam system for a controller obtained with NL_q stability constraints. The performance of the controller is comparable with that of an LQG controller, shown on the next figure (r_k:$\cdots$; u_k:-.-; $\hat{y}_k$: –).

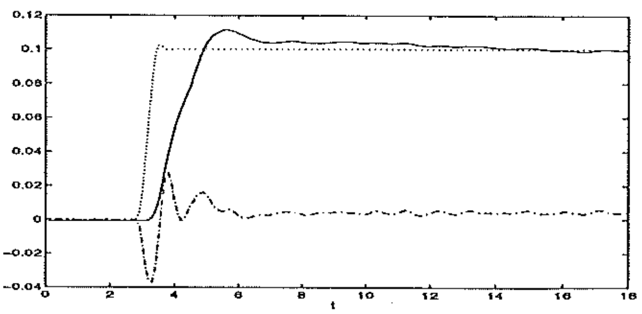

Figure 8: Step response of LQG controller, measured on the real system. The control signal is more nervous than on Fig. 7 (r_k:$\cdots$; u_k:-.-; $\hat{y}_k$: –).

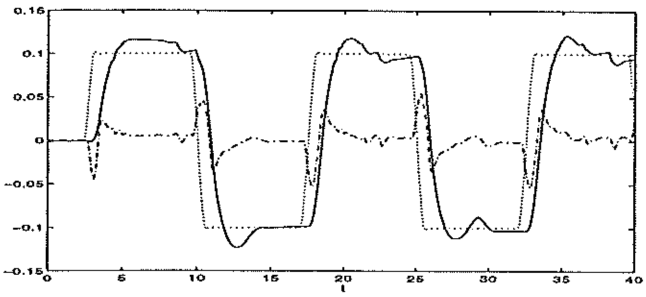

Figure 9: Same controller as on Fig. 7, tested on the real system for a square wave as reference input. The controller generalises successfully to this reference signal (r_k:···; u_k:-.-; $\hat{y}_k$: –).

7 Conclusion

In this paper we have shown that in designing linear output feedback controllers for the ball and beam system serious problems with closed-loop stability can arise when using Narendra's dynamic backpropagation procedure. By formulating the closed-loop system in NL_q representation form and by imposing NL_q internal or I/O stability constraints on dynamic backpropagation, the algorithm has been successfully modified in order to produce controllers for the ball and beam system that both on simulation and during testing on the real system show a performance comparable to LQG design.

References

[1] Billings S., Jamaluddin H., Chen S., "Properties of neural networks with applications to modelling nonlinear dynamical systems," *International Journal of Control*, Vol.55, No.1, pp.193-224, 1992.

[2] Boyd S., Barratt C., *Linear controller design, limits of performance*, Prentice-Hall, 1991.

[3] Boyd S., El Ghaoui L., Feron E., Balakrishnan V., *Linear matrix inequalities in system and control theory*, SIAM (Studies in Applied Mathematics), Vol.15, 1994.

[4] De Bie P., Motmans B., "Process control in practice: the ball and beam set up", K.U.Leuven, Belgium, Department of Electrical Engineering, ESAT-SISTA, *Technical Report, 92-63I*, 1992.

[5] Fletcher R., *Practical methods of optimization*, second edition, Chichester and New York: John Wiley and Sons, 1987.

[6] Narendra K.S., Parthasarathy K., "Gradient methods for the optimization of dynamical systems containing neural networks," *IEEE Transactions on Neural Networks*, Vol.2, No.2, pp.252-262, 1991.

[7] Suykens J.A.K., Vandewalle J.P.L., De Moor B.L.R., *Artificial Neural Networks for Modelling and Control of Non-Linear systems*, Kluwer Academic Publishers, Boston, Dec. 1995.

[8] Suykens J.A.K., De Moor B., Vandewalle J., "Nonlinear system identification using neural state space models, applicable to robust control design," *International Journal of Control*, Vol.62, No.1, pp.129-152, 1995.

[9] Suykens J.A.K., De Moor B., Vandewalle J., "Stability criteria for neural control systems," *European Control Conference ECC 95*, Roma Italy, Vol.3, pp.2766-2771, Sept. 1995.